15th Triennial World Congress, Barcelona, Spain

ELSEVIER
IFAC
PUBLICATIONS
www.elsevier.com/locate/ifac

INTERACTION OF AUTONOMOUS UNDERWATER VEHICLES WITH OCEAN STRUCTURES OF VARIABLE SIZE

Alberto Alvarez [*,1] **Andrea Caiti** [**]

[*] *North Atlantic Treaty Organization, SACLANT Undersea Research Centre, Viale San Bartolomeo, 400, 19138 La Spezia, Italy.*
[**] *ISME-DSEA, Department Electrical systems and Automation, University of Pisa, via Diotisalvi 2, 56100 Pisa, Italy*

Abstract: This work analyses the interaction of autonomous underwater vehicles (AUVs) with certain aspects of the ocean variability. Specifically, a simplified dynamical model of an AUV is integrated in ocean environments showing certain spatial variability. The length scales of the spatial structures are different for each environment and range from scales similar to the AUV to a hundred times bigger. Results indicate that the perturbations induced on the AUV by the environmental variability are stronger in the cases where the ocean structures are of similar size than the AUV. The strength of the perturbation decreases if the length scale of the spatial variability is increased. It was found that the perturbations induced by the environment on the AUV, are characterized by a power spectrum peaked at wavelengths half of the typical eddy size. *Copyright © 2002 IFAC*

Keywords: AUV, mission planning, eddies, ocean variability

1. INTRODUCTION

Unlike other robotic systems, autonomous underwater vehicles (AUVs) operate in frequently unknown ocean environments, characterized by complex variability (Schmidt and Bovio, 2000). The turbulent nature of the ocean implies that a wide range of spatial and time scales are continuously changing in the ocean. This variability, ranging from scales order of centimetres up to large scale ocean currents, can strongly perturb the development of AUVs operations (Galea, 1999). In consequence, determining and predicting ocean variability is a fundamental requirement to optimize certain aspects of the AUV's performance.

Numerical ocean models have been employed to provide nowcasts and forecasts of ocean variability (Holland and McWilliams, 1987). A typical numerical ocean model consists of finite difference equations representing the momentum, heat and salt balance in a determined area. These equations are integrated forward in time to predict the time evolution of the horizontal and vertical structure of the fluid flow as well as the temperature and salinity within the domain, given the wind stresses and buoyancy forcing at the sea surface. The grid or cell size in such calculations is crucial to determine the scales to be predicted. For example, to adequately resolve the typical 100-km-scale ocean eddies a 10-km resolution in a 10000-km ocean would be required. In the vertical direction, one might need up to 50 layers to treat adequately the time evolution of vertical structure in the flow. Physical and numerical considerations set the size of the time step in such finite difference models,

[1] Corresponding author

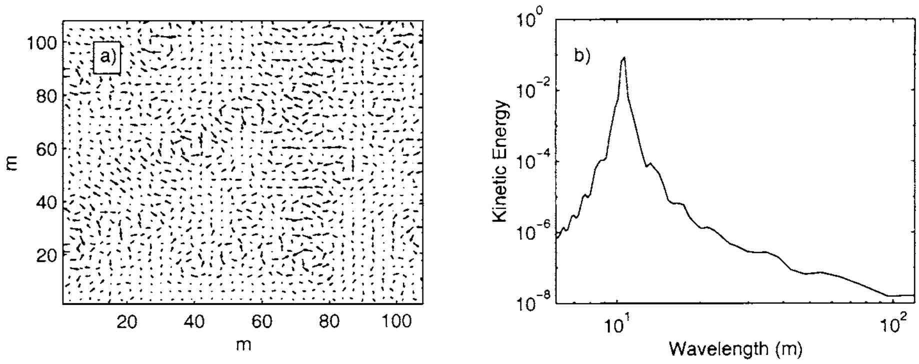

Fig. 1. a) Randomly generated current field with eddy structures of ≈ 10 m size. Only a section of 100×100 m^2 is shown for clarity. b) Power spectrum of the kinetic energy of the current field.

to a fraction of a day or perhaps even to tens of minutes.

While numerical ocean models can span a considerable part of ocean variability, their spatial resolutions are still hundreds to thousands times bigger than the characteristic size of an AUV. Thus, small scale ocean variability of the same spatial scale as AUVs (~ 1 m-10 m) is missed by numerical ocean models and predictions are not provided for the evolution of small scale structures. This lack of information constitutes a serious problem if strong momentum exchange between the AUV and small scale structures occurs.

This work attempts to elucidate which ocean scales interact with an AUV and, on the basis of the results obtained, to establish which scales should be predicted to plan safe missions. Section II describes the models employed to simulate the environment and the vehicle. Section III displays the results obtained from navigating an hypothetical AUV through different ocean environments characterized by dynamical structures of different size. Section IV concludes the work.

2. MODELING AND CONTROL

The case of AUV (1 m length and 0.3 m diameter) motion on the horizontal plane is considered. This simplification is justified by our interest in the effect of horizontal ocean structures on AUVs. Vertical motions in ocean structures are generally negligible and effects of waves on the AUV are beyond the scope of the present work. The dynamical model selected is sufficiently accurate to describe the dynamics of open-frame vehicles passively stable in pitch and roll (Caccia *et al.*, 2001). In the model the vehicle's position and orientation are referred to an inertial and environmentally-fixed reference frame. The linear and angular velocities are defined in a vehicle-fixed reference frame which, neglecting pitch and roll, is rotated an angle ψ on the horizontal plane with respect to the environmentally-fixed reference frame. The equations of motion are given by (Fossen, 1994; Campa *et al.*, 1999; Caccia *et al.*, 2001):

$$\dot{x} = u \cos\psi - v \sin\psi + \dot{x}_c \quad (1)$$

$$\dot{y} = u \sin\psi + v \cos\psi + \dot{y}_c \quad (2)$$

$$\dot{\psi} = r \quad (3)$$

$$m_u \dot{u} = m_v\, v\, r - k_{u|u|}\, u \mid u \mid + F_u \quad (4)$$

$$m_v \dot{v} = -m_u\, u\, r - k_{v|v|}\, v \mid v \mid \quad (5)$$

$$I_r\, \dot{r} = -(m_v - m_u)\, u\, v - k_{r|r|}\, r \mid r \mid + T_r \quad (6)$$

where u, v, and r are the surge, sway and yaw, respectively, m_u, m_v, and I_r are the vehicle masses and moment of inertia including added masses and inertia. The hydrodynamic damping is modelled as a quadratic term. A thruster is considered with its force applied along the surge direction, F_u. T_r is the torque in the yaw motion generated by a rudder located at the end of the vehicle. The angle that the rudder can deploy with respect to the longitudinal axis is bounded by maximum and minimum limits of $\pi/4$ and $-\pi/4$, respectively. A PD controller has been designed to keep the underwater vehicle in a straight path parallel to the x-coordinate. At each time the angle of the rudder δ with respect to the x-ccordinate in the body fixed frame is given by:

$$\delta = \alpha\, (y - y_p) + \beta\, \dot{y} \quad (7)$$

with $\alpha = -1$ m^{-1}, $\beta = 0.1$ s m^{-1} and y_p the y-coordinate of the straight line path in the environmentally fixed frame. Finally, $\dot{x}_c$ and $\dot{y}_c$ are the horizontal velocities of the flow.

Different current fields have been defined on a grid of 131×131 points. The distance between grid points corresponds to 3 m, so that the total system size is $L = 393$ m. The currents were obtained from a streamfunction field $\Psi(x, y)$ randomly generated from a specific isotropic power spectrum with random phases. The spectrum is peaked at

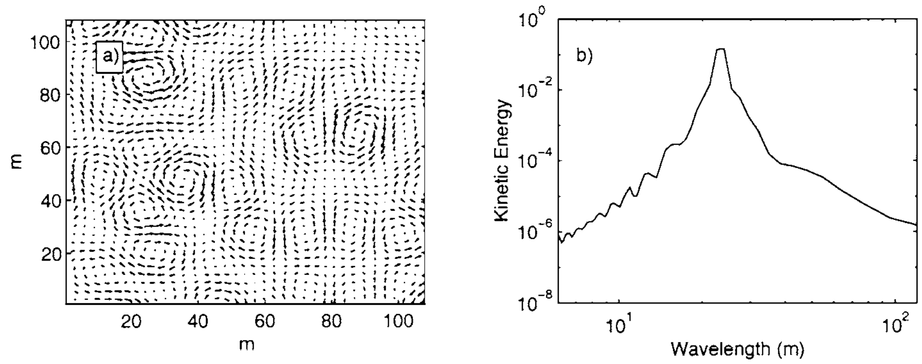

Fig. 2. a) Randomly generated current field with eddy structures of $\approx$ 20 m size. Only a section of 100×100 m^2 is shown for clarity. b) Power spectrum of the kinetic energy of the current field.

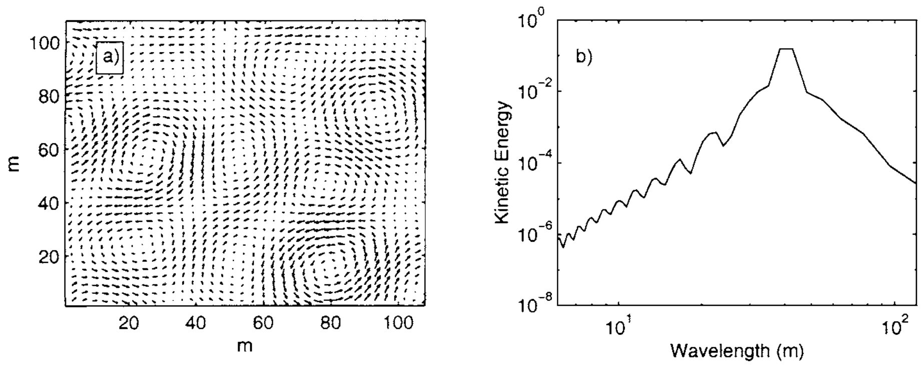

Fig. 3. a) Randomly generated current field with eddy structures of $\approx$ 40 m size. Only a section of 100×100 m^2 is shown for clarity. b) Power spectrum of the kinetic energy of the current field.

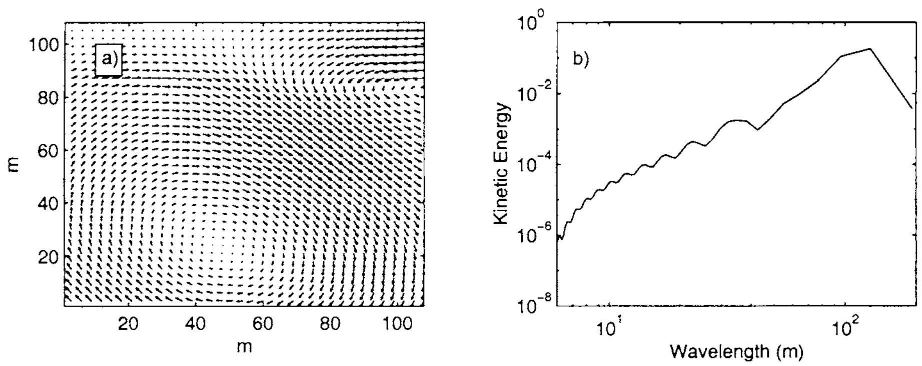

Fig. 4. a) Randomly generated current field with eddy structures of $\approx$ 100 m size. Only a section of 100×100 m^2 is shown for clarity. b) Power spectrum of the kinetic energy of the current field.

a determined spatial scale in order to obtain a field of eddies with homogeneous length scale. The velocity field is obtained from the streamfunction field from the relations:

$$\dot{x}_c = -\frac{\delta\Psi}{\delta y} \tag{8}$$

$$\dot{y}_c = \frac{\delta\Psi}{\delta x} \tag{9}$$

Maximum velocity of the flow in all generated current fields is 0.4 m/s.

3. RESULTS

Equations (1-6) have been numerically integrated in ocean environments with eddies of different length scales. Specifically, four cases with typical eddy sizes of 10 m (Figures 1a and b), 20 m (Figures 2a and b), 40 m (Figures 3a and b) and 100 m (Figures 4a and b) have been considered. An ensemble of ten simulations has been carried out for each current field. For each simulation, the initial location was randomly chosen in the y-coordinate and the AUV was controlled to follow a straight path crossing the current field in the x-

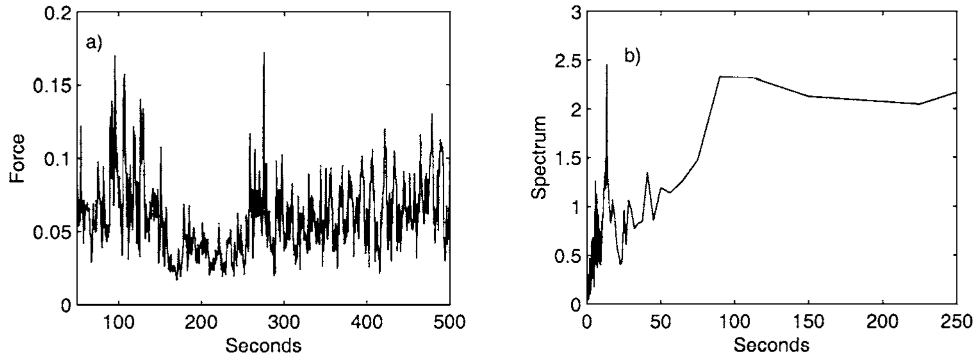

Fig. 5. a) Ensemble averaged of the random perturbations induced by an environment with eddy size $\approx 10\ m$. b) Average power spectrum of the perturbations.

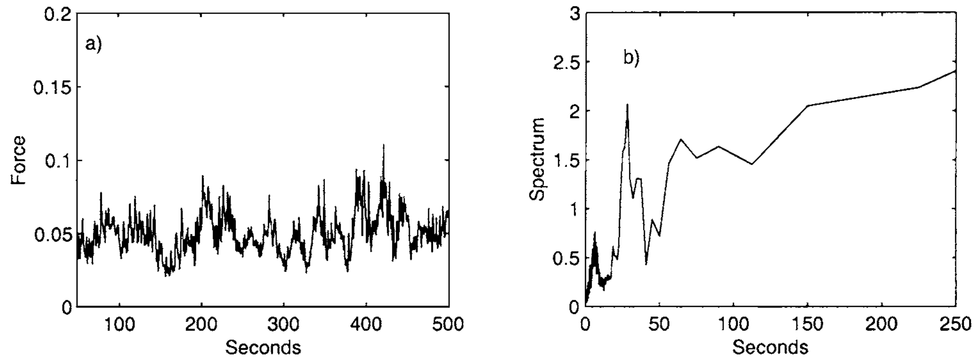

Fig. 6. a) and b) same as the previous but for the environment with eddy sizes $\approx 20\ m$.

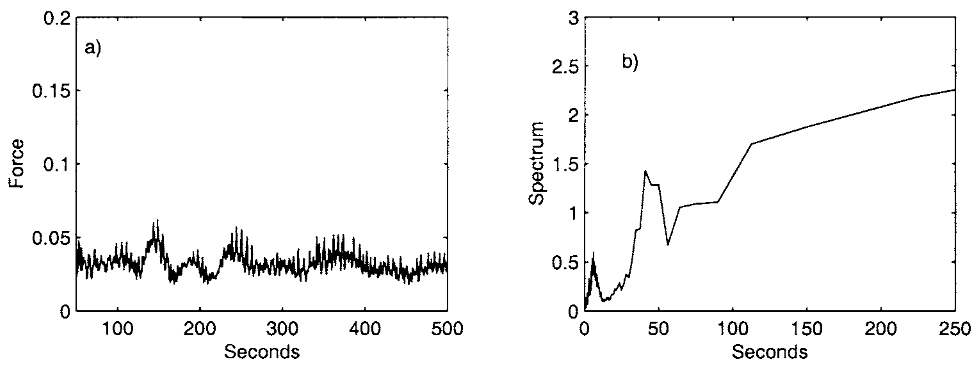

Fig. 7. a) and b) same as the previous but for the environment with eddy sizes $\approx 40\ m$.

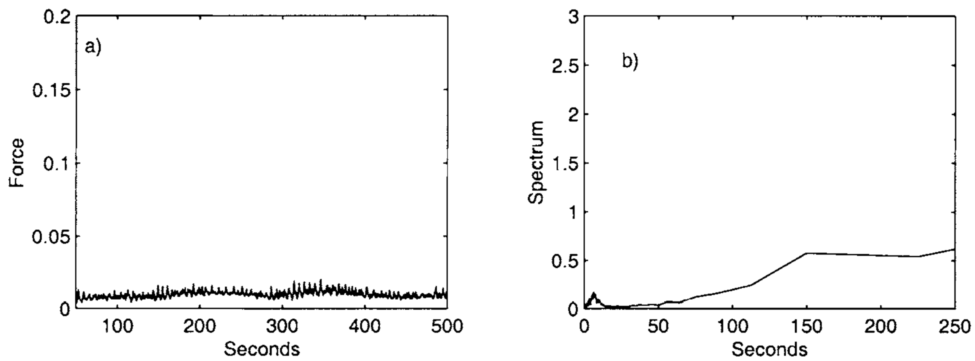

Fig. 8. a) and b) same as the previous but for the environment with eddy sizes $\approx 100\ m$.

direction. The navigation time was 500 s in all cases. During this time, no changes have been considered in the eddy field.

Figures 5a and b show the ensemble average of the unbalanced perturbations felt by the AUV and the power spectrum of the perturbations, in the case of an ocean environment with horizontal structures of around ten metres size. In Figure 5a, the force induced by the environment is computed from the time derivative of the momentum changes of the vehicle. Figure 5b reveals a peak in the spectrum of the perturbations corresponding to a period of 13 s. Considering that the average speed of the AUV was of $\approx$ 0.48 m/s, the time period corresponds to a spatial wavelength of $\approx 6\ m$, that is half size of the eddy size. Figure 6a shows that the amplitude of the perturbations decreases in an ocean environment with eddy sizes of $\approx$ 20 m, with respect to the previous case. The power spectrum shown in Figure 6b peaks at periods of 28 s corresponding to wavelengths of $\approx 13\ m$, half of the characteristic eddy size. Notice that the peak is less energetic and ill-defined than in the previous example. The decreasing tendency of the perturbations suffered by the AUV with the eddy size of the ocean structures is also observed for eddy sizes $\approx$ 40 m, Figures 8a and b. The power spectrum of the perturbations shows a peak at 41 s related to a wavelength of $\approx$ 20 m. No significant perturbations were found in the case of an ocean environment with ocean structures of $\approx 100\ m$.

4. CONCLUSIONS

The ocean is a dynamical system characterized by complex spatio-temporal variability. Its complexity arises from the fact that a wide range of spatial and time scales are dynamically linked in the ocean. In the last decade, attempts have been made to predict the components of ocean variability. Numerical ocean models have the capability to provide information about some aspects of the near future state of the ocean. However, their predictions are still limited to relatively large scale variability. Energetic flows induced by tides and small topographic perturbations, small scale instabilities and currents induced by local wind effects are some examples of ocean variability usually missed by numerical ocean models.

Prior knowledge of future ocean conditions would improve AUV mission planning. For example, attempts have been recently carried out to optimize the energy cost of an AUV mission using environmental information obtained from database or numerical ocean models (Carroll *et al.*, 1992; Alvarez and Caiti, 2001). While useful for some aspects of mission planning, the question remains if the information obtained from numerical models is sufficient to cover some fundamental issues as safety. To answer this question, a simplied dynamical model of an AUV has been integrated in ocean environments characterized by different eddy sizes, to determine which ocean scales interact most with an AUV. As expected from heuristic considerations, results indicate that ocean structures with length scales similar to the AUV, interacts strongly with the AUV. Conversely, the effects on the AUV of ocean structures with scales tens to hundreds bigger than the AUV size, are weak.

5. REFERENCES

Alvarez, A. and A. Caiti (2001). A genetic algorithm for autonomous underwater vehicle route planning in ocean environments with complex space-time variability. *Proceedings of the IFAC control applications of marine systems (CAMS 2001).*

Caccia, M., G. Bruzzone and G. Veruggio (2001). Experiments in the guidance of unmanned underwater vehicles. *Journal of the society for underwater technology* **24**, 143–151.

Campa, G., M. Innocenti and F. Nasuti (1999). Model of an underwater vehicle. *Internal report.*

Carroll, K. P., S. R. McClaran, E. L. Nelson, D. M. Barnett, D. K. Friesen and G. N. Williams (1992). Auv path planning: An a^* approach. *Proceedings of the symposium on AUV technology (AUV92)* pp. 3–8.

Fossen, T. I. (1994). *Guidance and control of ocean vehicles.* Wiley. Chichester.

Galea, A. M. (1999). Various methods for obtaining the optimal path for a glider vehicle in shallow water and high currents. *Proceedings of the* 11^{th} *international symposium on unmanned untethered submersible technology* pp. 150–161.

Holland, W. R. and J. C. McWilliams (1987). Computer modelling in physical oceanography from the global circulation to turbulence. *Physics Today* pp. 51–57.

Schmidt, H. and E. Bovio (2000). Underwater vehicle networks for acoustic and oceanographic measurements in the littoral ocean. *Proceedings of the 5th IFAC Conference Manoeuvring and Control of Marine Craft (MCMC2000)* pp. 323–326.